Available online at www.sciencedirect.com
ScienceDirect
Journal of Molecular Catalysis A: Chemical 277 (2007) 119–126
JOURNAL OF MOLECULAR CATALYSIS A: CHEMICAL
www.elsevier.com/locate/molcata

Low-temperature preparation and visible-light-induced catalytic activity of anatase F–N-codoped TiO_2

Yi Xie, Yuanzhi Li, Xiujian Zhao *

Key Laboratory of Silicate Materials Science and Engineering, Wuhan University of Technology, Ministry of Education, Wuhan, Hubei 430070, PR China

Received 3 June 2007; received in revised form 5 July 2007; accepted 6 July 2007
Available online 22 July 2007

Abstract

This paper reports a new process to prepare the F–N-codoped TiO_2 photocatalysts with anatase at 100 °C using $TiCl_4$ and NH_4F as titanium and fluorine, nitrogen sources, respectively. The as-prepared yellow or white yellow photocatalysts were characterized by X-ray diffraction (XRD), transmission electron microscopy (TEM), scanning electron microscopy (SEM), nitrogen adsorption/desorption measurements (BET), X-ray photoelectron spectroscopy (XPS) and UV–vis diffuse reflectance spectra (UV–vis DRS). The results showed that the F–N-codoping extended the absorbance spectra of TiO_2 into visible region. The BET surface area of the as-prepared F–N-codoped TiO_2 photocatalyst was high up to 191 $m^2\ g^{-1}$. The results of degradation of methyl orange (MO) solution showed that the F–N-codoped samples exhibit much higher visible-light-induced catalytic activities than that of Degussa P25 and the as-prepared pure TiO_2. This property can be attributed to the synergetic effects of absorption in the visible-light region, red shift in adsorption edge, good crystallization, porous structure and large surface area of the F–N-codoped TiO_2.

Keywords: Low-temperature preparation; F–N-codoping; Titanium dioxide; Visible light

1. Introduction

In the past decades, TiO_2 has been the most widely used and investigated photocatalyst because of its nontoxicity, inexpensiveness, chemical stability and favorable optoelectronic properties. However, it can only work under ultraviolet (UV) light (wavelength $\lambda < 388$ nm) due to its wide bandgap of 3.0–3.2 eV, which means only ~4% of the incoming solar energy on the surface can be utilized. As a result, the widespread technological use of TiO_2 photocatalyst has been hampered. Many attempts have been made to improve the optical response of TiO_2 under visible-light excitation. In recent years, nonmetal doping of TiO_2 rekindled a great interest in visible-light catalysis since the report of the work of Asahi et al. in 2001 [1]. Since then, both the preparation methods and the theoretical calculations have been performed and reported for nonmetal doping of TiO_2 [2–18].

A large number of techniques have been employed to prepare F/N-doped TiO_2 photoactive in the visible range, including sputtering [1,9], chemical vapor deposition [10], sol–gel [11–13], ion implantation [14,15] and spray pyrolysis (SP) [16,17], etc. Yu et al. prepared F-doped TiO_2 by sol–gel and they proposed that the doped F atoms convert Ti^{4+} to Ti^{3+} by charge compensation and F atoms occupied the crystal sites of the TiO_2 lattice by replacing oxygen atoms, which enhanced the photocatalytic activity [11]. As for the F–N–TiO_2 system, the first report on N–F-codoped TiO_2 is made by Nukumizu et al. [18], who prepared $TiN_xO_yF_z$ with a bandgap-absorption edge at ~570 nm using $(NH_4)_2TiF_6$, SiO_2 and NH_3 as sources. Li et al. [16] prepared F–N-codoped TiO_2 powders with new absorption bands in the visible range of 400–550 nm and they found that the powder synthesized at the temperature of 1173 K was superior to that of commercial P25. Liu and co-workers [19] also prepared F–N-codoped TiO_2 by sol–gel-solvothermal method and this type of photocatalysts showed higher photocatalytic activity in the visible range than that of P25, N-doped TiO_2 and F-doped TiO_2. However, these experiments were performed at high temperatures, typically from 300 to 600 °C, which usually resulted in the increase of the crystallite size and lowering of the surface areas,

* Corresponding author. Tel.: +86 27 8765 2553; fax: +86 27 8766 9729.
E-mail addresses: xieyithanks@163.com (Y. Xie), opluse@whut.edu.cn (X. Zhao).

1381-1169/$ – see front matter © 2007 Elsevier B.V. All rights reserved.
doi:10.1016/j.molcata.2007.07.031

and thus hampered the enhancement of photocatalytic activity. To our knowledge, the preparation of F–N-codoped TiO_2 by the sol–gel route at low temperature, which will overcome the two drawbacks mentioned above, has rarely been reported.

In this paper, we describe a detailed study of synthesis of F–N-codoped TiO_2 powders, changing the dosage of starting materials NH_4F. The experimental results revealed that the codoping of TiO_2 with F and N not only extended the optical absorption spectrum into visible range, but also exhibited high visible-light activity in the degradation of methyl orange (MO) aqueous solution. The present method may open a new horizon for preparation of nonmetal-doped TiO_2 photocatalysts to use in the organic compounds degradation under visible irradiation.

2. Experimental

2.1. Synthesis

$TiCl_4$ (Sinopharm Chemical Reagent Co. Ltd., China), diluted ammonia (1:9), H_2O_2 (30%) and NH_4F (Shanghai Shiyi Chemicals Reagent Co. Ltd., China) were used for the synthesis. All of the chemicals are analytical grade. The starting material NH_4F was used to introduce fluorine and nitrogen. Distilled water was used throughout this study. The process diagram for sol–gel synthesis of F–N-codoped TiO_2 photocatalysts is shown in Fig. 1. Typically, 18 mL of $TiCl_4$ was added dropwise into 1500 mL distilled water in an ice-water bath with strong magnetic stirring. After 30 min, the pH of this acidic solution was adjusted to 7 by dropwise addition of diluted ammonia solution. After stirring at this pH for 24 h, the obtained white precipitates were filtered and washed thoroughly with distilled water repeatedly until Cl^- was not detected. Thereafter the precipitates were ultrasonic dispersed in 1500 mL distilled water. H_2O_2 (140 mL) was added dropwise into this mixture under stirring. The resulting yellow semitransparent solution was divided into six portions. One portion was heated at 100 °C for 24 h and the resulting light yellow solution was dried at 60 °C to prepare pure TiO_2 and to calculate the concentration of TiO_2. A certain amount of NH_4F dissolved in 50 mL of distilled water was added to each of the above solutions. Then, the mixtures were heated at 100 °C for 4 h in a temperature controlled oil bath equipped with a magnetic stirrer, thermometer and reflux condenser. The amount of NH_4F was changed to compare the effect of different molar ratio of NH_4F/TiO_2. Finally, the resulting light yellow or pale precipitates were dried at 60 °C for 24 h and grinded in agate mortar to obtain the powder samples. To prepare F–N-codoped titania with different composition of N and F, the dosage of NH_4F was changed.

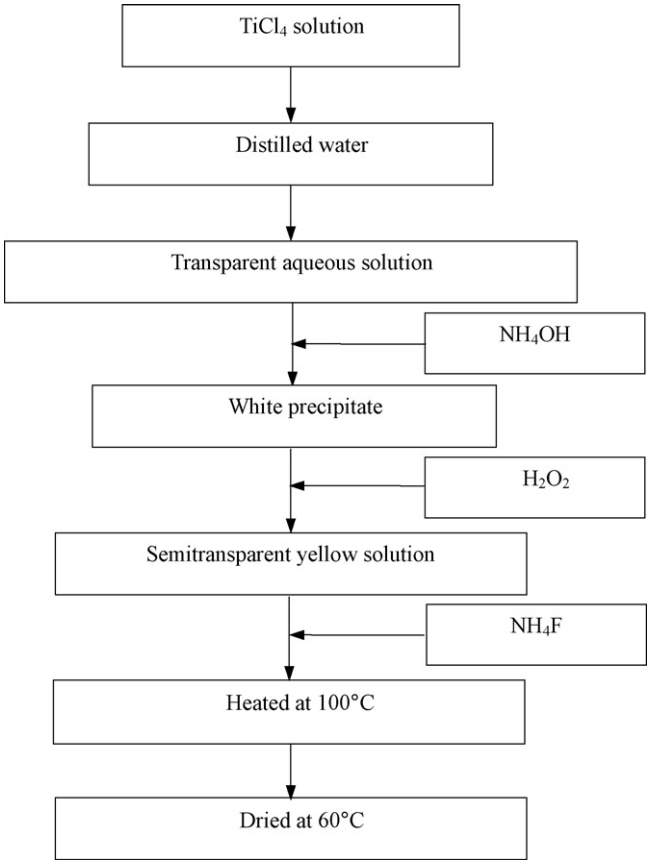

Fig. 1. Process diagram for preparation of F–N-codoped TiO_2 photocatalysts.

2.2. Characterization

The X-ray diffraction (XRD) of the as-prepared F–N-codoped TiO_2 was carried out in a D/MAX-βA (Rigaku, Japan) diffractometer using Cu Kα radiation at 40 kV and 50 mA in the region of $2\theta = 20$–$80°$. Crystallite size and morphology of the F–N-codoped TiO_2 particles were examined by scanning electron microscopy (SEM) (JSM-5610LV, JEOL LTD., Japan) and transmission electron microscopy (TEM) on a JEM-2010 (Japan) microscope operating at 200 kV in the mode of bright field. The UV–vis diffuse reflectance spectra (UV–vis DRS) were recorded on a UV–vis spectrophotometer (UV-2550, Shimadzu, Japan) with an integrated sphere attachment. The analyzed range was 200–700 nm, and $BaSO_4$ was used as the reflectance standard. The Brunauer–Emmett–Teller (BET) surface areas (S_{BET}) of the selected F–N-codoped TiO_2 photocatalysts were analyzed in an AUTOSORB-1 (Quantachrome Instruments, USA) nitrogen adsorption apparatus. All the samples were degassed at 100 °C prior to actual measurements. The S_{BET} was determined by a multipoint BET method using the adsorption data in the relative pressure (P/P_0) range of 0.05–0.25. Desorption isotherm was used to determine the pore size distribution via the Barret–Joyner–Halender (BJH) method with cylindrical pore size [20]. X-ray photoelectron spectroscopy (XPS) measurements were performed on an ESCALAB MK II spectrometer (VG Scientific Ltd., UK) with nonmonochromatic Al Kα X-ray (1486.6 eV). The pressure in the chamber during the experiments was about 10^{-7} Pa. The analyzer was operated at 50 eV pass energy for high resolution spectra and 100 eV for survey spectra. The binding energy of the C 1s line (284.6 eV) was taken for calibrating the obtained spectra. Background subtraction and peak fitting was performed using a public XPS peak fit program (XPSPEAK4.1 by R. Kwok). Recorded spectra were fitted using Gauss–Lorentz curves and the Lorenz–Gauss ratio for each Ti, O, F and N species was kept constant.

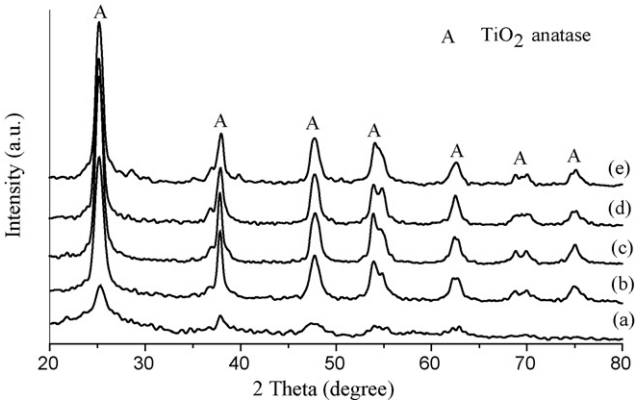

Fig. 2. XRD patterns of F–N-codoped TiO_2 as-prepared with different starting NH_4F/TiO_2 molar ratios: (a) 1/5; (b) 1/2; (c) 1/1; (d) 2/1; (e) 4/1.

2.3. Photocatalytic evaluation

Photocatalytic activity of the as-prepared photocatalysts and Degussa P-25 TiO_2 was evaluated by the degradation of methyl orange (MO) aqueous solution in a 100 mL beaker reactor. In a typical experiment, 120 mg of powders was added into 30 mL of MO solution with a concentration of 10 mg L^{-1}. The suspensions were magnetically stirred for 20 min in the dark to establish the equilibrium of MO adsorption/desorption followed by switching on light. Photodegradation of MO was performed at room temperature by using a high pressure Hg-light (125 W) with the UV cut-off filter. The UV cut-off filter was placed between the beaker and light source to exclude ultraviolet radiation under 420 nm. The incident intensity to the sample surface was 214 μW cm^{-2}. At the given intervals, a few mL of the suspensions were drawn from the beaker, and filtered by centrifugation. Its UV-vis spectra were recorded on a UV–vis spectrophotometer (UV-1601, Rigaku, Japan). The relative concentration of MO was monitored by comparing its absorbance at 464 nm with that of the original solution. The measured solutions were returned to the original vial for subsequent irradiation experiments. Multiple photocatalysis experiments were performed under the identical reaction conditions to confirm the reproducibility.

3. Results and discussion

3.1. Crystal structure

Fig. 2 shows the XRD patterns of as-prepared F–N-codoped TiO_2 samples. The distinctive peaks at $2\theta = 25.18°$, 37.84°, 47.76°, 54.06°, 62.44°; corresponding to the anatase (1 0 1),

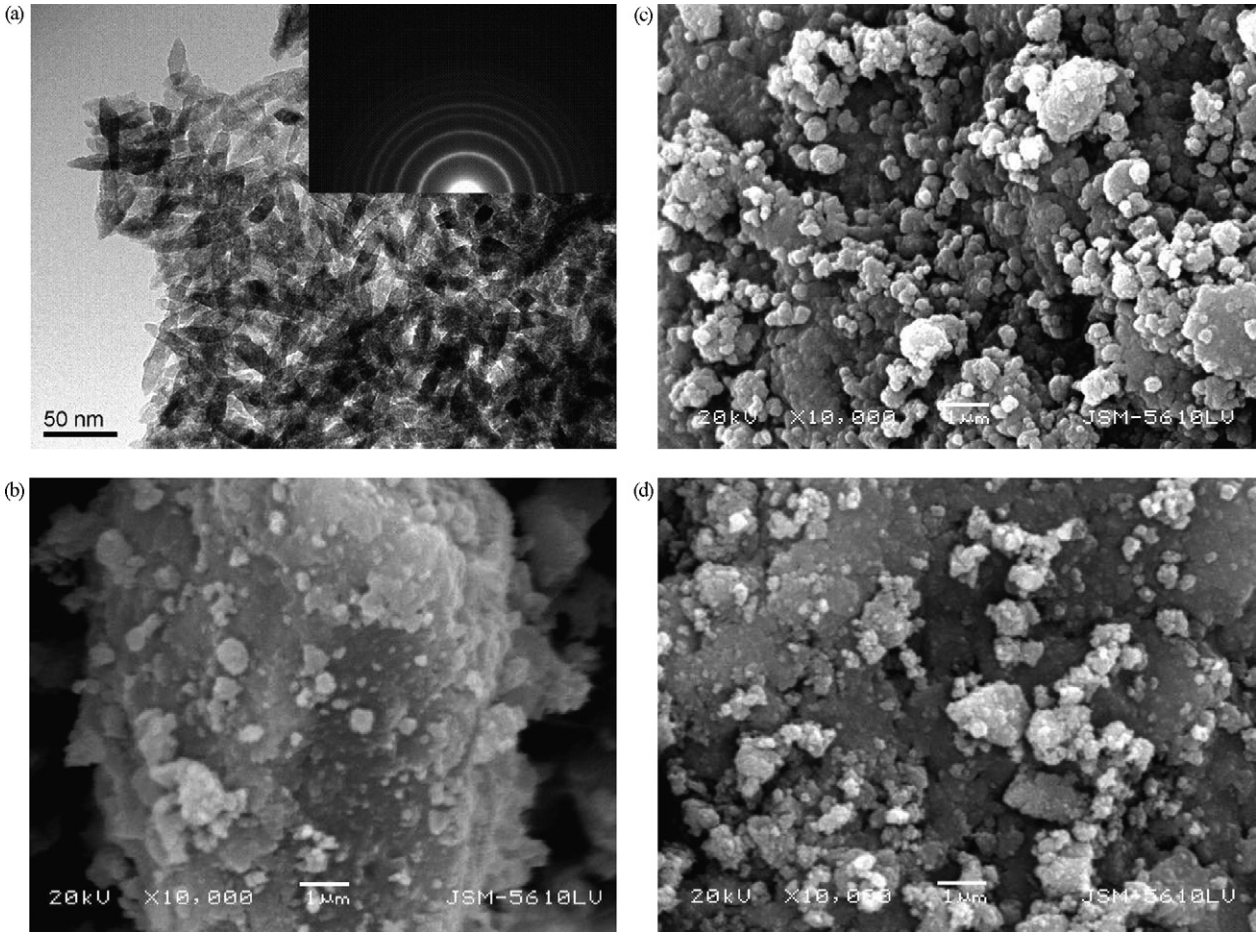

Fig. 3. TEM image and SAED pattern (inset) of sample as-prepared with NH_4F/TiO_2 molar ratio of 1/2 (a) and SEM images of samples as-prepared with different starting NH_4F/TiO_2 molar ratios of 1/5 (b), 1/2 (c) and 2/1 (d).

(1 0 3, 0 0 4 and 1 1 2), (200), (1 0 5 and 2 1 1), (2 0 4) crystal planes (PDF: 21-1272) are observed in all the samples heated at 100 °C for 10 h. Usually, the amorphous-anatase transformation may complete in the temperature range from 250 to 400 °C, while anatase TiO_2 with a small amount of brookite has been prepared even at 40 °C [17]. The peak positions are nearly the same and no extra peaks except for anatase TiO_2 are observed, suggesting that the structure of TiO_2 is not changed. Compared to pure TiO_2, the codoped photocatalysts show a slight shift of the (1 0 1) peak, indicating a lattice distortion of the doped photocatalysts [4]. Crystal lattice distortion is reported to be important for absorption edge shift towards the visible-light region [21].

The structure of F–N-codoped TiO_2 powders was further studied by TEM image and selective area electron diffraction (SAED) (inset, Fig. 3). It can be seen that the present wet method produced F–N-codoped TiO_2 crystals with rodlike shapes (length:width ratio of ~5:1). For example, heat treatment of solution with initial F/Ti molar ratio of 1:2 produced uniform: ~50 nm × 10 nm particles. The phase structure of the sample TFN2 was also confirmed to be anatase by SAED analysis. Fig. 3b–d shows SEM micrographs of the F–N-codoped TiO_2. The powders are found to be fine and slightly agglomerated. Sample TFN2 displays porous structure, creating void volumes in the photocatalysts. This structure along with large effective surface area is beneficial to enhancing the adsorption of reactants.

3.2. BET surface areas and pore structure

Fig. 4 shows the nitrogen adsorption–desorption isotherms for the as-prepared F–N-codoped TiO_2 photocatalysts. Except for sample TFN1, all the other samples exhibit the hysteresis loop similar to a type IV isotherm, which are characteristics of mesoporous materials [22]. The pore size distribution curve calculated from the desorption branch of the nitrogen isotherm by the Barrett–Joyner–Halenda (BJH) method shows that the pore size distributions become narrower with increasing amount of reagent NH_4F (Fig. 5). The estimated textural parameters such as specific surface area (S_{BET}), total pore volume (V_p) for different samples are also compiled in Table 1. As seen, the diameter of mesopore is from 3.9 to 7.5 nm and the BET surface area initially increases with increasing molar ratio of NH_4F/TiO_2 and decreases when the ratio is higher than 1/1. The sample TFN3 with starting NH_4F/TiO_2 molar ratio of 1/1 presented a large S_{BET} value of 191 $m^2\ g^{-1}$, much higher than that of most N/F-doped TiO_2 reported in the literatures [5,19,23,24]. Therefore, we can conclude that the present wet chemical process

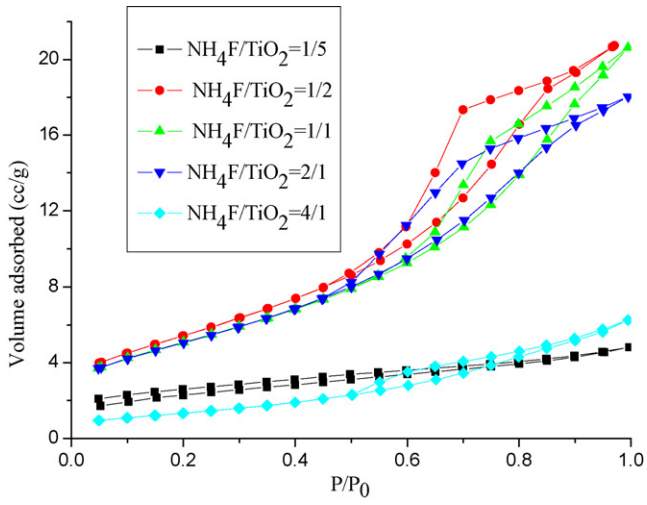

Fig. 4. N_2 adsorption–desorption isotherms of as-prepared F–N-codoped TiO_2 photocatalysts with different starting NH_4F/TiO_2 molar ratios.

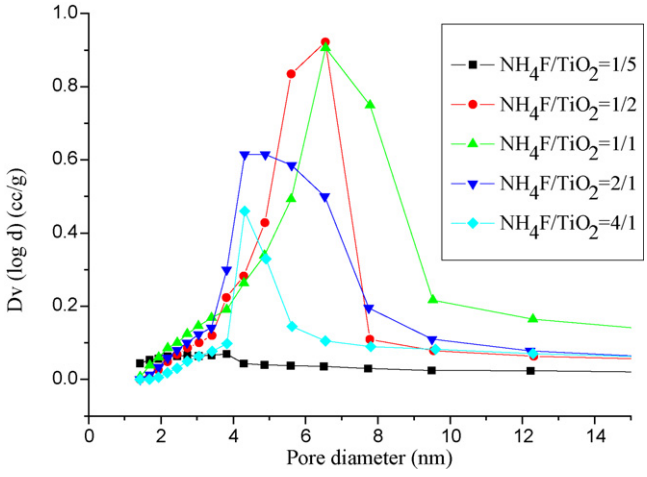

Fig. 5. BJH desorption pore size distribution of as-prepared samples with different starting NH_4F/TiO_2 molar ratios.

is a good route for preparation of porous photocatalyst with high surface area. This conclusion is favorable in enhancing the photocatalytic activity of TiO_2-based photocatalyst since these mesopores allow rapid diffusion of various reactants and products during photocatalytic reaction [11].

3.3. XPS analysis

The XPS was carried out to determine the chemical composition of the as-prepared samples and the valence states of

Table 1
Preparation conditions and other physical parameters of the as-prepared F–N-codoped TiO_2

Sample	NH_4F/TiO_2 molar ratio	BET surface area (S_{BET}) ($m^2\ g^{-1}$)	Average pore diameter (nm)	Total volume (V_p) ($cm^3\ g^{-1}$)	Band gap
TFN1	1/5	74	3.9	0.069	2.44
TFN2	1/2	145	6.4	0.233	2.97
TFN3	1/1	191	6.9	0.328	3.18
TFN4	2/1	156	6.0	0.236	3.19
TFN5	4/1	64	7.5	0.124	3.20

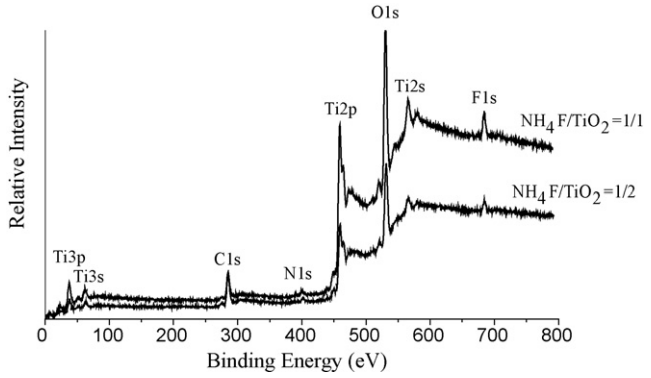

Fig. 6. XPS survey spectrum of samples as-prepared with starting NH_4F/TiO_2 molar ratios of 1/2 (TFN2) and 1/1 (TFN3).

various species present therein. XPS survey spectra show that the F–N-codoped TiO_2 photocatalysts contain predominantly Ti, O, N and F elements and a trace amount of carbon (Fig. 6). The photoelectron peak for Ti 2p appears at a binding energy of 459 eV, that for O 1s at 530 eV, that for F 1s at 685 eV, that for N 1s at 400 eV and that for C 1s at 285 eV. The XPS peak for C 1s is due to the surface pollution from air and the adventitious hydrocarbon from the XPS instrument, and not discussed here.

Fig. 7 represents the high-resolution XPS spectra of the Ti 2p, O 1s, F 1s and N 1s region, taken on the samples prepared with starting NH_4F/TiO_2 molar ratio of 1/5 (sample TFN2) and 1/2 (sample TFN3). The results by curve fitting are shown in Table 2. As indicated in Table 2, oxygen is deficient in a stoichiometric ratio. The total content of N in sample TFN3 is 4.51 at.%, higher than that in sample TFN2 (2.18 at.%). The amount of F in TFN3 is estimated to be 11.22 at.%, much higher than that in TFN2 (2.72 at.%).

The spin–orbit components ($2p_{3/2}$ and $2p_{1/2}$) of Ti 2p peaks are well deconvoluted by two curves at 458.7 (458.5) and 464.4 (464.2) eV (Fig. 7a) with a split of 5.7 eV between the doublets, indicating that Ti exists in the Ti^{4+} form [25]. The O 1s signal for sample TFN2 and TFN3 is shown in Fig. 7b. By curve fitting, the peak at 530.50 (530.25) eV corresponds to lattice oxygen of TiO_2, and a shoulder located at higher binding energy of 531.9 eV is assigned to mixed contributions from surface hydroxides [26,27].

Many researchers reported that fluorine and nitrogen species induce visible-light absorption and response [16–19]. To investigate the states of fluorine and nitrogen on the as-prepared samples, the F 1s and N 1s core levels were also measured by XPS (Fig. 7c and d). The F 1s region is composed of two contributions. The main contributions at 685.1–685.2 eV are similar with the attributions to the F atoms in $TiOF_2$ [16,17], but in our result, no obvious $TiOF_2$ phase was observed in the XRD pattern (Fig. 2). They can be assigned to F^- ions physically adsorbed on the surface of samples [11]. The minor contributions at 687.5 eV attributed to the doped F atoms in TiO_2, which is similar with that of some literatures [16,17]. The N 1s XPS spectra of samples TFN1 and TFN3 shown in Fig. 7d also reveal a large broadness, which can be deconvoluted by two peaks with the binding energies at 400.4 and 402.0–402.1 eV. The N 1s XPS spectrum at binding energy around 396 eV was generally considered the evidence for the presence of Ti–N bonds [1,28]. However, the assignment of the N 1s peaks ranging in the 398–403 eV is still under debate. The N 1s XPS peaks at 398.2 [5], 400 [29] and 401.5 eV [30] were assigned to the formation of the N–Ti–O linkages. However, the peaks at 400 ± 0.2 [14], 401 [4] and 402 eV [31] were assigned to the molecularly chemisorbed γ-N state. Additionally, the N 1s core level at 400 [32] and 400.2 eV [33] for the N-doped TiO_2 were attributed to NO-like species. The differences discussed above may be due to the differences of preparation procedure. The nitrogen state in the doped TiO_2 may vary from case to case and variations in the XPS results may be associated with the different surface structures [34]. Considering the consistency with the results of the DFT calculations [15], we attribute the N 1s at 400.4 and 402.0–402.1 eV shown in Fig. 7d as NO_x species.

3.4. UV–vis spectra

The corresponding UV–vis DRS for the as-prepared F–N-codoped TiO_2 photocatalysts are provided in Fig. 8. Pure TiO_2 has no ability to respond to visible light, whereas the codoping of nitrogen and fluorine extends the absorption edges to the visible-light region. The intensity of the visible-light absorption decreases with increasing amount of starting reagent NH_4F. Comparatively, Nukumizu et al. [18] has prepared F–N-codoped titania with a bandgap-absorption edge at ~570 nm. Li et al. [16] also prepared F–N-codoped TiO_2 powder with new absorption bands in the visible range of 400–550 nm. Here, sample TFN1 with starting NH_4F/TiO_2 of 1/5 exhibits the largest visible-light absorption in the five samples, and its absorption edge shifts to 600 nm. The difference in absorption edge wavelength for different F–N-codoped TiO_2 photocatalysts clearly indicates the band gap of the various samples. By evaluating, the plots of trans-

Table 2
Results of curve fitting of the high-resolution XPS spectra for the Ti 2p, O 1s, F 1s and N 1s regions

Sample	Ti		O		F		N	
	Ti ($2p_{3/2}$)	Ti ($2p_{1/2}$)	Bulk O^{2-}	OH	F^-	$TiO_{2-x}F_x$	NO_x	
TFN2								
BE (eV)	458.7	464.4	530.5	532.2	685.2	687.5	400.4	402.0
Content (at.%)	28.93		56.37	9.80	2.43	0.29	0.86	1.32
TFN3								
BE (eV)	458.5	464.2	530.25	532.2	685.1	687.5	400.4	402.1
Content (at.%)	23.03		40.24	21.00	10.42	0.80	1.51	3.00

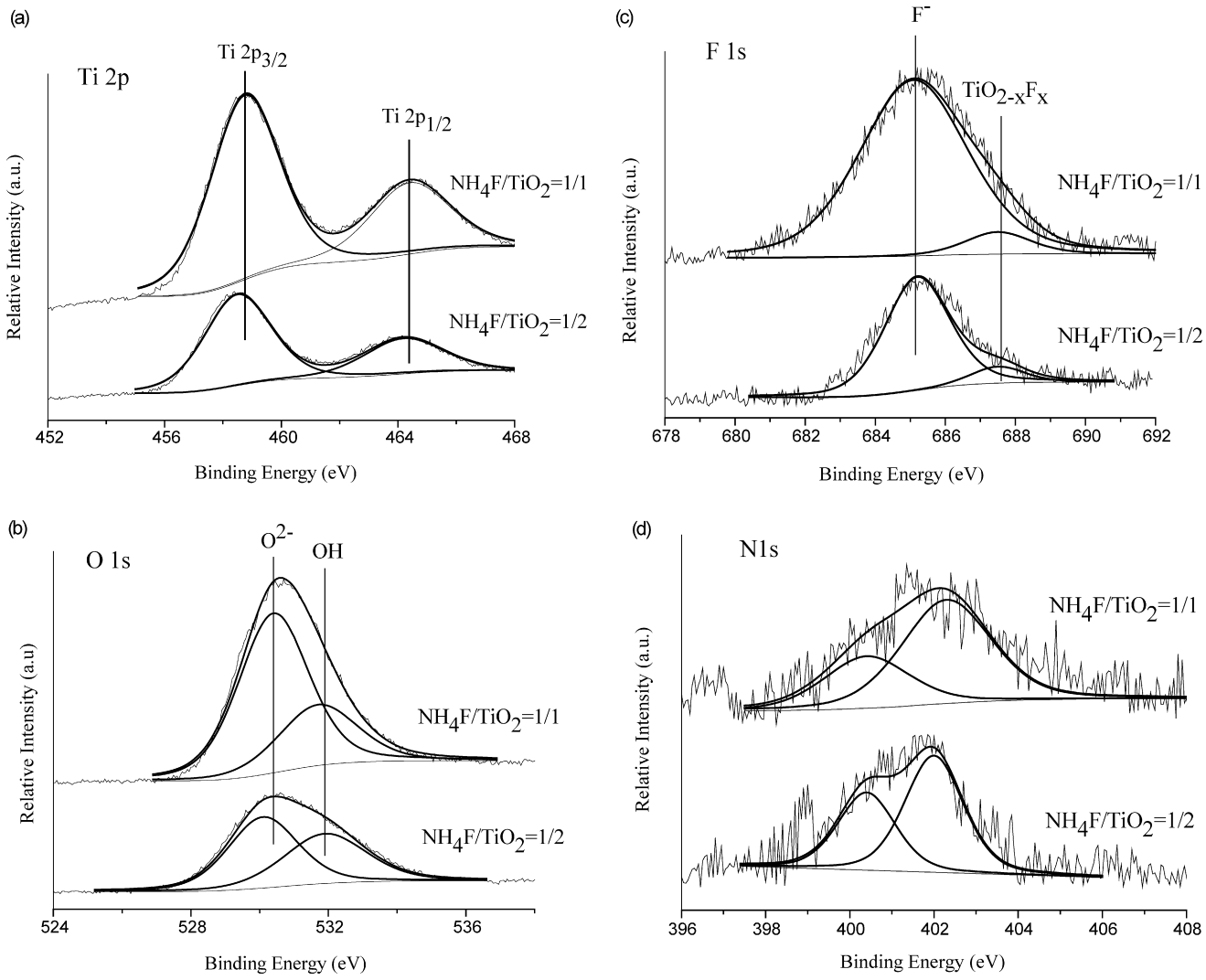

Fig. 7. Ti 2p (a), O 1s (b), F 1s (c) and N 1s (d) high-resolution XPS spectra of samples as-prepared with starting NH_4F/TiO_2 molar ratios of 1/2 (TFN2) and 1/1 (TFN3).

formed Kubelka–Munk function versus the band gap energy for the as-prepared F–N-codoped TiO_2 photocatalysts are shown in Fig. 7b, from which the corresponding band-gap energies can be obtained [35,36] and summarized in Table 1. The band-gap energies of samples prepared with starting NH_4F/TiO_2 molar ratio of 1/5 and 1/2 are estimated 2.44 and 2.97 eV, respectively, typically in the visible-light region.

3.5. Photocatalytic activity

Fig. 9 shows the visible-light-induced photocatalytic decomposition of MO with F–N-codoped TiO_2 photocatalysts. It can be seen that the dosage of starting NH_4F affects the photocatalytic activity. Among them, the F–N-codoped TiO_2 with starting molar ratio of NH_4F/TiO_2 1–2 showed the highest photodegradation activity with a MO conversion of 94.5% after 6 h irradiation, which was two and six times higher than that by commercial P25 TiO_2 and pure TiO_2, respectively. F-doped [17] or N-doped [10] TiO_2 was reported to show high visible-light-induced catalytic efficiency and F–N-codoping was found to greatly improve the visible-light-induced activity for decomposition acetaldehyde [16] or *p*-chlorophenol [19]. In our case, mono-doped TiO_2 by fluorine or nitrogen was not discussed since both of F and N were detected from XPS even when small amount of reagent NH_4F was used. These results indicate that F–N-codoping is an effective way to improve the visible-light-induced photocatalytic activity of TiO_2-based catalysts for decomposition of organic compounds.

The degradation of MO solution on the commercial P25 and as-prepared pure TiO_2 could be based on the photosensitization process of dyes under visible-light irradiation [37]. The photocatalytic activity of TiO_2-based photocatalyst is due to the production of excited electrons in the conduction band and positive holes in the valence band, irradiated by the absorption of UV or visible illumination. Practically, the activity of a photocatalyst is affected by many factors such as surface area, crystallinity, surface hydroxyl density and oxygen vacancies [38]. At wavelengths $\lambda \geq 420$ nm, the intensity of absorption spectra is different for all the samples. At the same light intensity of 214 $\mu W\,cm^{-2}$, the lower the utilization of light energy for

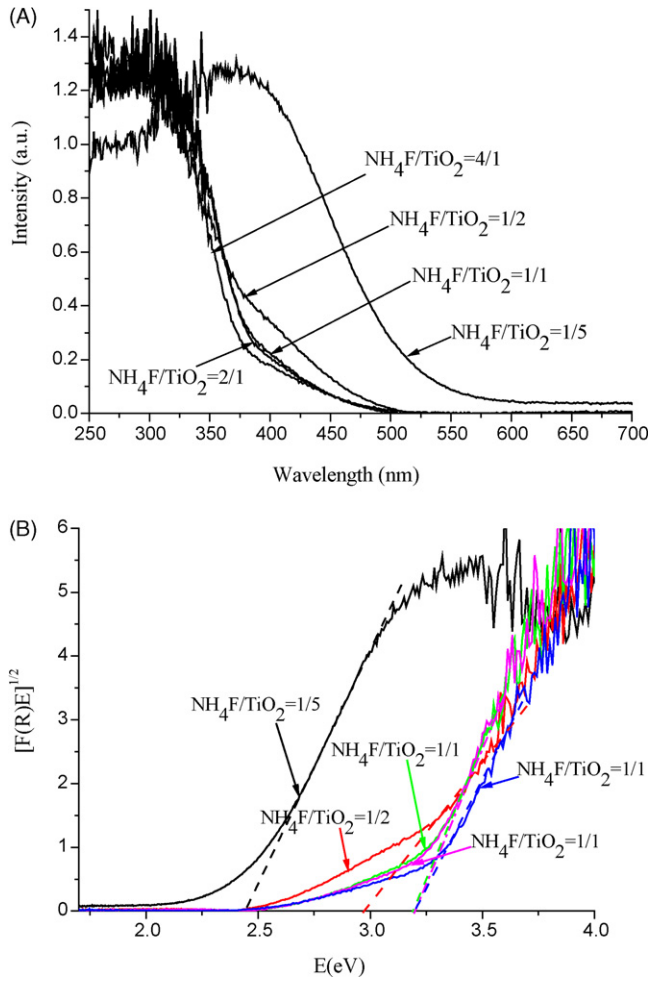

Fig. 8. UV–vis diffuse reflectance spectra (A) and a plot of the transformed Kubelka–Munk function vs. the energy of the light absorbed (B) of F–N-codoped TiO_2 photocatalysts as-prepared with different starting NH_4F/TiO_2 molar ratios.

visible light, the slower the decomposition rate of MO solution. In addition, the surface area and crystalline size are different, resulting in the different recombination rate of electron–hole pair. The porous structure shown in Fig. 3c is beneficial to enhancing the adsorption of MO, which improves the photocatalytic activity. Overall, the high visible-light-induced catalytic activity is attributed to the synergetic effects of strong absorption in the visible-light region, red shift in adsorption edge, good crystallization, porous structure and large surface area of the F–N-codoped TiO_2. It should be noted that there is not a definite correlation between the light absorption properties and the activity of the samples, that is, the stronger the absorption of visible-light dose not mean the higher the decomposition rate of MO, typically comparing the photocatalytic and adsorption properties of sample TFN1 with those of sample TFN2.

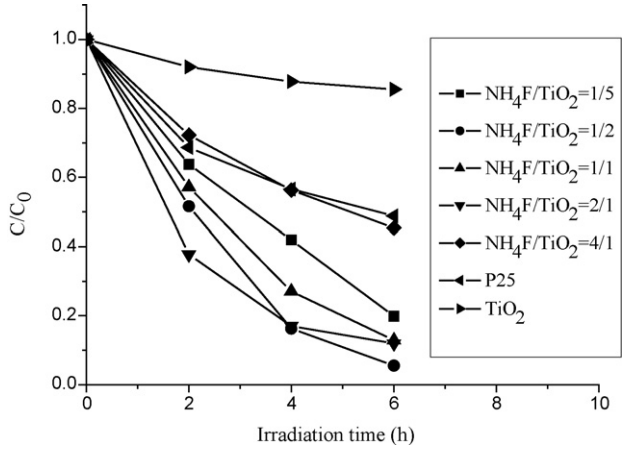

Fig. 9. Photocatalytic decomposition profiles of MO solution over F–N-codoped TiO_2 as-prepared with different starting NH_4F/TiO_2 molar ratios, pure TiO_2 and P25 TiO_2.

4. Conclusions

F–N-codoped TiO_2 photocatalysts with anatase were prepared at low temperature for the first time. Particularly, physical and photocatalytic properties of photocatalysts prepared with different starting molar ratio of NH_4F to TiO_2 have been compared with each other. Compared with pure TiO_2, UV–vis DRS of the F–N-codoped TiO_2 photocatalysts showed a shift towards higher wavelengths, with absorbance edges up to 600 nm. BET surface area was affected by the dosage of NH_4F, and the photocatalysts with starting NH_4F/TiO_2 ratio of 1/1 showed the surface area as large as 191 $m^2\,g^{-1}$. The F–N-codoped TiO_2 could show significant photocatalytic activity under visible-light irradiation ($\lambda \geq 420$ nm), much higher than that of pure TiO_2 and Degussa P25. Overall, the process of codoping nitrogen and fluorine though wet process at low temperature is prominent for preparation of nonmetal-doped TiO_2 with high surface area and high visible-light-induced catalytic activity.

Acknowledgements

This research was financial supported by the Program for Changjiang Scholars and Innovative Research Team in University (PCSIRT, No. IRT0547) and the Cultivation Fund of the Key Scientific and Technical Innovation Project (No. 705036), Ministry of Education.

References

[1] R. Asahi, T. Morikawa, T. Ohwaki, A. Aoki, Y. Taga, Science 293 (2001) 269–271.
[2] S. Khan, M. Al-Shanhry, W.B. Ingler, Science 297 (2002) 2243–2245.
[3] S. Joung, T. Amemiya, M. Murabayashi, K. Itoh, Chem. Eur. J. 12 (2006) 5526–5534.
[4] J. Yuan, M.X. Chen, J.W. Shi, W.F. Shangguan, Int. J. Hydrogen Energy 31 (2006) 1326–1331.
[5] M. Sathish, B. Viswanathan, R.P. Viswanath, C.S. Gopinath, Chem. Mater. 17 (2005) 6349–6353.
[6] H.Q. Sun, Y. Bai, Y.P. Cheng, W.Q. Jin, N.P. Xu, Ind. Eng. Chem. Res. 45 (2006) 4971–4976.
[7] C. Di Valentin, G. Pacchioni, A. Selloni, Chem. Mater. 17 (2005) 6656–6665.
[8] J.C. Yu, W. Ho, J. Yu, H. Yip, P.K. Wong, J. Zhao, Env. Sci. Technol. 39 (2005) 1175–1179.

[9] J.M. Mwabora, T. Lindgren, E. Avendaño, T.F. Jaramillo, J. Lu, S.-E. Lindquist, C.-G. Granqvist, J. Phys. Chem. B 108 (2004) 20193–20198.
[10] Y. Guo, X.W. Zhang, G.R. Han, Mater. Sci. Eng. B 135 (2006) 83–87.
[11] J.C. Yu, J.G. Yu, W.K. Ho, Z.T. Jiang, L.Z. Zhang, Chem. Mater. 14 (2002) 3808–3816.
[12] R. Bacsa, J. Kiwi, T. Ohno, P. Albers, V. Nadtochenko, J. Phys. Chem. B 109 (2005) 5994–6003.
[13] C. Di Valentin, G. Pacchioni, A. Selloni, S. Livraghi, E. Giamello, J. Phys. Chem. B 109 (2005) 11414–11419.
[14] A. Ghicov, J.M. Macak, H. Tsuchiya, J. Kunze, V. Haeublein, L. Frey, P. Schmuki, Nano Lett. 6 (2006) 1080–1082.
[15] A. Nambu, J. Graciani, J.A. Rodriguez, Q. Wu, E. Fujita, J. Fdez Sanz., J. Chem. Phys. 125 (2006) 094706.
[16] D. Li, H. Haneda, S. Hishita, N. Ohashi, Chem. Mater. 17 (2005) 2588–2595.
[17] D. Li, H. Haneda, S. Hishita, N. Ohashi, N.K. Labhsetwar, J. Fluorine Chem. 126 (2005) 69–77.
[18] K. Nukumizu, J. Nunoshige, T. Takata, J.N. Kondo, M. Hara, H. Kobayashi, K. Domen, Chem. Lett. 32 (2003) 196–197.
[19] D.G. Huang, S.J. Liao, J.M. Liu, Z. Dang, L. Petrik, J. Photochem. Photobiol. A 184 (2006) 282–288.
[20] K.S.W. Sing, D.H. Everett, R.A.W. Haul, L. Moscou, R.A. Pierotti, J. Rouquerol, T. Siemieniewska, Pure Appl. Chem. 57 (1985) 603.
[21] T. Ohno, M. Akiyoshi, T. Umebayashi, K. Asai, T. Mitsui, M. Matsumura, Appl. Catal. A: Gen. 265 (2004) 115–121.
[22] J.G. Yu, M.H. Zhou, B. Cheng, X.J. Zhao, J. Mol. Catal. A: Chem. 246 (2006) 176–184.
[23] S. Yin, K. Ihara, Y. Aita, M. Komatsu, T. Sato, J. Photochem. Photobiol. A 179 (2006) 105–114.
[24] K. Demeestere, J. Dewulf, T. Ohno, P.H. Salgado, H.V. Langenhove, Appl. Catal. B-Env. 61 (2005) 140–149.
[25] B.M. Reddy, K.N. Rao, G.K. Reddy, P. Bharali, J. Mol. Catal. A: Chem. 253 (2006) 44–51.
[26] E. McCafferty, J.P. Wightman, Surf. Interface Anal. 26 (1998) 549.
[27] B. Erdem, R.A. Hunsicker, G.W. Simmons, E. David Sudol, V.L. Dimonie, M.S. El-Aasser, Langmuir 17 (2001) 2664–2669.
[28] K. Kobayakawa, Y. Murakami, Y. Sato, J. Photochem. Photobiol. A 170 (2005) 177–179.
[29] J.S. Jang, H.G. Kim, S.M. Ji, S.W. Bae, J.H. Jung, B.H. Shon, J.S. Lee, J. Solid State Chem. 179 (2006) 1067–1075.
[30] X. Wang, J.C. Yu, Y. Chen, L. Wu, X. Fu, Env. Sci. Technol. 40 (2006) 2369–2374.
[31] Y.C. Hong, C.U. Bang, D.H. Shin, H.S. Uhm, Chem. Phys. Lett. 413 (2005) 454–457.
[32] S. Sato, R. Nakamura, S. Abe, Appl. Catal. A 284 (2005) 131–137.
[33] H. Chen, A. Nambu, W. Wen, J. Graciani, Z. Zhong, J.C. Hanson, E. Fujita, J.A. Rodriguez, J. Phys. Chem. C 111 (2007) 1366–1372.
[34] P. Xu, L. Mi, P.N. Wang, J. Cryst. Growth 289 (2006) 433–439.
[35] B. Karvaly, I. Hevesi, Z. Naturforsch Teil A 26 (1971) 245–249.
[36] S. Sakthivel, H. Kisch, Angew Chem. Int. Ed. 42 (2003) 4908.
[37] T. Wu, G. Liu, J. Zhao, H. Hidaka, N. Serpone, J. Phys. Chem. B 103 (1999) 4862–4867.
[38] M.A. Fox, M.T. Dulay, Chem. Rev. 93 (1993) 341.